HHS Public Access

Author manuscript

Nucl Med Biol. Author manuscript; available in PMC 2016 November 01.

Published in final edited form as:

Nucl Med Biol. 2015 November ; 42(11): 880–886. doi:10.1016/j.nucmedbio.2015.07.008.

Tumor and organ uptake of ^{64}Cu-labeled MORAb-009 (amatuximab), an anti-mesothelin antibody, by PET Imaging and biodistribution studies

Jae-Ho Lee[1,*], **Heejung Kim**[1], **Zhengsheng Yao**[1], **Sung-Jin Lee**[1], **Lawrence P Szajek**[2], **Luigi Grasso**[3], **Ira Pastan**[4], and **Chang H Paik**[1,*]

[1]Nuclear Medicine, Radiology and Imaging Sciences, Clinical Center, NIH, Bethesda, MD 20892, USA

[2]Positron Emission Tomography Department, Clinical Center, NIH, Bethesda, MD 20892, USA

[3]Morphotek, Inc, Exton, PA, USA

[4]Laboratory of Molecular Biology, NCI, NIH, Bethesda, MD 20892, USA

Abstract

Objectives—To investigate the effect of the injection dose of MORAb-009 (amatuximab, an anti-mesothelin monoclonal antibody), the tumor size and the level of shed mesothelin on the uptake of the antibody in mesothelin-positive tumor and organs by biodistribution (BD) and positron emission tomography (PET) imaging studies.

Methods—2-S-(4-isothiocyanatobenzyl)-1,4,7-triazacyclononane-1,4,7-triacetic acid (p-SCN-Bn-NOTA) was conjugated to amatuximab and labeled with $^{64}CuCl_2$ in 0.25M acetate buffer, pH 4.2. The resulting ^{64}Cu-NOTA-amatuximab was purified with a PD 10 column. To investigate the dose effect or the effect of tumor size, the BD was performed in groups of nude mice (n=5) with mesothelin-expressing A431/H9 tumors (range, 80~300 mm^3) one day after iv injection of ^{64}Cu-NOTA-amatuximab (10 μCi) containing a total amatuximab dose of 2, 30, or 60 μg. The BD and PET imaging were also investigated 3, 24 and 48 h after injecting a total dose of 30 μg (10 μCi for BD), and 2 or 60 μg (300 μCi for PET), respectively.

Results—Comparing the results of the BDs from three different injection doses, the major difference was shown in the uptake (% ID/g) of the radiolabel in tumor, liver and blood. The tumor uptake and blood retention from 30 and 60 μg doses were greater than those from 2 μg dose, whereas the liver uptake was smaller. The BD studies also demonstrated a positive correlation between tumor size (or the level of shed mesothelin in blood) and liver uptake. However, there was a negative correlation between tumor size (or the shed mesothelin level) and tumor uptake and between tumor size and blood retention. These findings were confirmed by the PET imaging

[*]Corresponding author: Tel.: +1 301 496 1426; fax: +1 301 402 4548. leejaeho@mail.nih.gov (JH Kee, PhD), cpaik@mail.nih.gov (Chang H. Paik, PhD).

study, which clearly visualized the tumor uptake with the radiolabel concentrated in the tumor core and produced a tumor to liver ratio of 1.2 at 24 h post-injection with 60 μg amatuximab, whereas the injection of 2 μg amatuximab produced a tumor to liver ratio of 0.4 at 24 h post-injection.

Conclusion—Our studies using a nude mouse model of A431/H9 tumor demonstrated that the injection of a high amatuximab dose (30 to 60 μg) could provide a beneficial effect in maximizing tumor uptake while maintaining minimum liver and spleen uptakes of the radiolabel, and in facilitating its penetration into the tumor core.

Keywords

^{64}Cu labeling; NOTA; mesothelin; amatuximab; antibody; tumor targeting

1. Introduction

Positron emission tomography (PET) offers high resolution and sensitivity combined with the unique ability to measure tissue concentrations of radioactivity in three dimensions [1–5]. Radiolabeling of an antibody with radio-metal PET isotopes such as ^{64}Cu (t1/2, 12.7 h) and ^{89}Zr (t1/2, 78.4 h) is an emerging approach for immuno-PET imaging because their longer decay half-lives are suitable for studying the tumor uptake of biological molecules such as monoclonal antibodies (mAbs) [6–13]. In this study we used ^{64}Cu to label MORAb-009. Amatuximab is a high affinity chimeric (mouse/human) antibody that shares 82.6% amino acid sequence identity to a human IgG1κ and is directed against mesothelin [14, 15]. Mesothelin, an immunogenic membrane glycoprotein of 40 kDa, is over-expressed in many epithelial cancers (almost 100% of all pancreatic adenocarcinomas and mesotheliomas, in > 65 % of ovarian adenocarcinomas, and in many non-small cell lung cancers) and has limited expression in normal tissues [16, 17]. Mesothelin is internalized actively into the cell's cytosol and is shed from the tumor cell surface, generating soluble mesothelin in the tumor's interstitial space, which can also be detected in circulation [18, 19]. We previously conjugated MORAb-009 with a bifunctional chelator, CHX-A″, for radiolabeling with ^{111}In [14]. Previously, ^{111}In-CHX-A″-MORAb-009 has been evaluated preclinically and in clinical studies [17, 20].

To enhance radioimmunodetection sensitivity we are interested in the use of ^{64}Cu-NOTA-amatuximab. This ^{64}Cu labeled amatuximab may enable us to accurately quantify tumor and organ uptakes of amatuximab using PET/CT and provide dosimetric determinations quantitatively before therapy. ^{64}Cu–mAb radiolabeling has been tested for many antibodies. In this study, ^{64}Cu labeling of amatuximab was carried out after the conjugation of a bifunctional chelator, *p*-SCN-Bn-NOTA with high metal-chelate stability. The targeting of mesothelin-specific tumors can be hampered by shed mesothelin because it can act as a decoy to the tumor targeting of amatuximab. On the other hand, shed mesothelin can provide useful information on tumor stage and tumor treatment efficacy [21, 22]. Herein, we report our studies on the effects of amatuximab dose, tumor size and the concentration of shed mesothelin on tumor and major organ uptake values of ^{64}Cu-labeled amatuximab measured by biodistribution and PET imaging studies, thereby optimizing the injection dose

of unconjugated amatuximab to achieve a high tumor uptake in a nude mouse model of mesothelin-expressing A431/H9 tumors.

2. Materials and methods

2.1. Reagents

Amatuximab was obtained from Morphotek, Inc. (Exton, PA). 2-S-(4-isothiocyanatobenzyl)-1,4,7-triazacyclononane-1,4,7-triacetic acid (*p*-SCN-Bn-NOTA) was purchased from Macrocyclics, Inc. (Dallas, TX). ^{64}Cu was produced *via* the ^{64}Ni(p,n)^{64}Cu nuclear reaction using a cyclotron at the National Institutes of Health (NIH, Bethesda, MD).

2.2. Conjugation of p-SCN-Bn-NOTA to amatuximab

Amatuximab (M.W., 144.33 kDa; 0.027mM, 4 mg/mL) was conjugated with 2-S-(4-isothiocyanatobenzyl)-1,4,7-triazacyclononane-1,4,7-triacetic acid (*p*-SCN-Bn-NOTA) (4 mM in dimethyl sulfoxide) at a molar ratio of 1:4 in 0.1 M sodium bicarbonate at pH 9.5 and 25°C for 5 hours. The NOTA-amatuximab conjugate was purified with a size exclusion PD 10 column (GE Healthcare Bio-Sciences AB, Uppsala, Sweden) and filtered through a Microcon® filter with a 30 kDa cutoff (Millipore, Bedford, MA). The column and filter were pretreated with 100 μL of BSA (25 mg/mL) and 100 μL of DTPA (1 mM) to remove potential metal contaminants, and then washed with metal free 0.25 M sodium acetate (pH 5.5). The concentration of the mAb was measured according to the method of Bradford [23]. The level of NOTA molecules conjugated per amatuximab was estimated by the distribution of ^{64}Cu between the peaks representing amatuximab and free NOTA separated by the HPLC analysis after the conjugation product mixture was radiolabeled using the method described below.

2.3. Radiolabeling

Purified NOTA-amatuximab (1.0 mg/1 mL, 6.7 μM) was labeled with ^{64}Cu in 100 μL solution containing sodium acetate (0.25 M) buffer (pH=4.2) and d-mannitol (20 mg/mL) at 25°C for 1 h. EDTA at a final concentration of 3 mM was then added to the reaction solution to bind potential free ^{64}Cu ions. The labeled product was analyzed with size exclusion HPLC equipped with a size exclusion TSK gel G3000SW column (7.8 x 300 mm, 5 μm, TOSOH Bioscience, Japan; 0.067 M sodium phosphate/0.15 M sodium chloride, pH 6.8; 1.0 mL/min), a UV monitor, and an on-line flow radioactivity detector (Bioscan Inc., Washington, DC) to obtain the radiolabeling yield. The radiolabeling yield (>70%) was determined based on the distribution of ^{64}Cu between ^{64}Cu labeled NOTA-amatuximab (retention time, 9 min) and unbound ^{64}Cu (retention time, 14 min) in the HPLC profiles. The labeled product was purified with a PD 10 column eluted with PBS. A radiochemical purity of > 95% was used for the biodistribution and PET imaging studies. The specific activity was about 55 μCi/μg of amatuximab.

2.4. Immunoreactivity determination

The immunoreactivity of ^{64}Cu-NOTA-amatuximab was determined by modifying the cell-binding assay of Lindmo, et al. [24]. Aliquots (5 ng/50 μL) of the conjugated samples were incubated side-by-side with an increasing number of A431/H9 (mesothelin-positive human

epidermoid carcinoma cells obtained from Dr. Ira Pastan, NCI) (2 x 10^4-1 x 10^6) in 100 μL of PBS with 1% BSA at 4°C for 3 h. Nonspecific binding to the cells was determined by performing the cell-binding assays under conditions of antibody excess (25 μg amatuximab). The maximum specific cell-bound counts, corrected for non-specific binding and expressed as a percentage of the total count, were taken as the immunoreactivity. The immunoreactivity of ^{64}Cu-NOTA-amatuximab was 80.1±10.7 % (N=3).

2.5. Tumor model

A431/H9 cells (5 x10^6 mesothelin molecules expressed on the surface of each cell) were used to make an *in vivo* tumor model. A431/H9 cells were cultured as previously described [25]. Briefly, A431/H9 cells were grown in DMEM medium supplemented with 10% FBS, 750 μg/mL geneticin (G418) and 1% penicillin-streptomycin under a humidified atmosphere with 5% CO_2. Tumor xenografts were established by inoculation of 2 x 10^6 cells in 0.1 mL PBS subcutaneously into the right or left hind flank of athymic mice (NCI-DCT, Frederick, MD) for BD studies. For PET imaging studies, the mice were inoculated with 2 x 10^6 cells in 0.1 mL PBS subcutaneously into the left shoulder of athymic mice.

2.6. Biodistribution studies

For the BD studies, ^{64}Cu-labeled amatuximab conjugate with 1.6 NOTA molecules per amatuximab was used. Groups (n = 5 mice/group) of mice were injected intravenously with ^{64}Cu-labeled amatuximab conjugate mixed with unlabeled amatuximab (2, 30, 60 μg total) in 0.2 mL PBS containing 1% BSA when the tumor sizes were approximately 200 mm^3 (range, 80~300 mm^3). The unlabeled amatuximab was co-injected to block shed-mesothelin in the blood. The animals were euthanized at 3, 24, and 48 h by CO_2 inhalation and exsanguinated by cardiac puncture before dissection. Blood and various organs were removed and weighed, and their decay corrected radioactivity counts were measured with a gamma-counter (Wallac, Inc., Perkin-Elmer, Inc., Boston, MA). The percentage of injected dose per gram (% ID/g) of the blood or each organ was calculated and normalized to a 20-gram mouse. All animal experiments were performed under a protocol approved by the NIH Animal Care and Use Committee.

2.7. PET imaging

Longitudinal PET scans were performed on athymic mice (n=5) using a Siemens Inveon micro PET scanner (Siemens Preclinical Solutions, Knoxville, TN) at 3, 24, and 48 h post-injection (p.i.)[26]. All imaging procedures were performed under anesthesia with 1.5% isoflurane in oxygen at 2 L/min. Tumor-bearing mice were injected with 0.3 mCi of ^{64}Cu-labeled amatuximab conjugate with unlabeled amatuximab (2 or 60 μg total) in 0.2 ml of normal saline intravenously through the tail vein and 15 min static PET scans were performed at 3, 24, and 48 h p.i. The mice were euthanized after the imaging session. The images were reconstructed with a 3-dimensional ordered-subset expectation maximization/maximum a posteriori (OSEM3D/MAP) algorithm, with no attenuation or scatter correction. The reconstructed pixel size was 0.77 × 0.77× 0.79 mm on a 128 × 128 × 159 imaging matrix. Tumors were manually segmented and each image analysis was performed using ASIPRO software (provided by Siemens, v6.8.0.0) on decay-corrected whole-body images.

To characterize the accumulation of the probe in tumors, the region-of-interest (ROI) were drawn manually on individual tumor area, liver, spleen, muscle, and heart. The %ID/g was calculated for mice at 3, 24, and 48 h p.i. Activity concentration (cps/voxel) was determined by maximum pixel value and was then converted to μCi/cc using a cross calibration factor. Activity concentration (μCi/cc) was divided by injected dose to get the image derived percent injected dose (%ID/g) assuming the tissue density as 1 g/ml.

2.8. Statistical Analysis

Statistical analysis was performed using ANOVA to compare multiple groups, and the Student's *t* test was performed for unpaired data between two groups. All tests were two-sided, and a probability value (*p*) of less than 0.05 was considered significant.

3. Results

3.1. Biodistribution studies

In this study, we used a nude mouse model of A431/H9 tumor (range, 80~300 mm^3). We first investigated the effect of co-injected amatuximab dose on the uptake of ^{64}Cu-NOTA-amatuximab (10μCi) in tumor, blood and organs at 24 h. We found a substantial increase in the tumor uptake (9.0±2.6 for 2 μg vs.17.7±4.4 %ID/g for 30 μg, p=0.02 and 16.4±4.6 %ID/g for 60 μg, p=0.02) and blood retention (5.1±1.0 for 2 μg vs. 12.9±3.7 %ID/g for 30 μg, p=0.06 and 10.0±0.7 %ID/g for 60 μg, p<0.003), but lower liver uptake (30.8±5.6 for 2 μg vs. 16.2±3.2 %ID/g for 30 μg, p<0.002 and 15.9±3.3 %ID/g for 60 μg, p<0.002) of ^{64}Cu-NOTA-amatuximab as the amatuximab dose was increased from 2 μg to 30 μg or 60 μg (Fig. 1a).

We also investigated the biodistribution of ^{64}Cu-NOTA-amatuximab with a total amatuximab dose of 30 μg at different time points to assess the peak uptake time and the peak uptake value since the total dose of 30 μg produced good tumor uptake at 24 h (Fig.1b, Table 1). The radiolabeled amatuximab cleared gradually from blood while accumulating in tumor with its peak uptake (17.7±4.4 %ID/g) at 24 h p.i. As per organ uptake, the radiolabel was primarily taken up by liver, spleen and kidneys. The tumor-to-organ and tumor-to-blood ratios increased over time with the ratios greater than 1 at 24 h, indicating the visualization of tumor would be feasible by PET imaging at this time point with the 30 μg dose.

The effect of tumor size on the tumor, blood and organ uptake of ^{64}Cu-NOTA- amatuximab was also investigated at 24 h p.i. for each co-injected amatuximab dose. The results indicate that tumor uptake was inversely correlated with tumor size (R-squared value: 0.37 for 2 μg, 0.77 for 30 μg, 0.92 for 60 μg) (Fig. 2). Of note, higher variations in tumor size caused higher standard deviations in tumor uptake values in Fig. 1 even within the same experiment set. Liver uptake showed positive correlation with tumor size and the blood uptake had an inverse correlation with tumor size.

3.2. PET imaging studies

When tumor size reached about 200 mm^3 (range, 170 to 320 mm^3) 7 days after the inoculation, PET imaging studies were performed at 3, 24 and 48 h post-injection of 0.3 mCi

of ^{64}Cu-NOTA-amatuximab with 2 μg and 60 μg amatuximab dose to confirm the dose effect shown in the BD studies (Fig.3). The PET images visualized tumors as early as 3 h p.i. for both 2 and 60 μg amatuximab dose. At this time, the major radioactivity was shown in heart (blood pool), liver and spleen for both 2 and 60 μg amatuximab injections and the radioactivity signal was also present in the lower abdomen especially for 2 μg injection, indicating that a significant percentage of the injected dose was excreted via both the hepatobiliary and renal systems for 2 μg injection. At 24 and 48 h p.i., the radioactivity signal in the tumor remained relatively unchanged compared to that at 3 h p.i. for 2 μg whereas the tumor signal at later time points was much stronger than that at 3 h p.i. for 60 μg, indicating that this higher injection dose is advantageous for the tumor visualization by PET. Both transverse and coronal PET images clearly displayed tumor uptake that was diffused into the center of the tumors for both 2 and 60 μg amatuximab injections. The tumor and organ uptake values were determined by the region-of-interested analysis (ROI) on PET images (Fig.4). Comparing the effect of two different injection doses on tumor, blood and organ uptakes of the radiolabel, the radioactivity of 2 μg injection cleared more rapidly from the blood than that of 60 μg injection (34.4±4.4 vs. 33.7±1.8 %ID/g at 3 h, 5.4±1.3 vs. 13.1±1.5 %ID/g, $P<0.001$ at 24 h, and 2.4±0.5 vs. 7.6±2.6 %ID/g, $p<0.01$ at 48 h). This difference in blood clearance was reflected in a higher tumor uptake (25.4±6.5 vs. 13.2±1.8 %ID/g, $p=0.01$) and lower liver uptake (21.9±3.3 vs. 31.5±6.5 %ID/g, $p=0.03$) for 60 μg injection at 24 h p.i. than for 2 μg injection. The tumor-to-liver ratio for 60 μg (Table 2) showed a value > 1 at 24 and 48 h p.i., whereas the ratios for 2 μg dose at the same time points was < 1, indicating that it is feasible to visualize tumors in the upper abdomen with the higher injection dose.

4. Discussion

Amatuximab was labeled with ^{64}Cu using a NOTA derivative as a bifunctional chelator instead of the corresponding DOTA derivative because ^{64}Cu-NOTA mAb was reported to be more stable than the corresponding ^{64}Cu-DOTA conjugate *in vivo* [27]. It was reported that A431/H9 tumors shed soluble mesothelin into the interstitial space and blood circulation with its concentrations linearly proportional to the tumor size [28]. Since shed mesothelin can act as a decoy preventing anti-mesothelin antibodies from targeting mesothelin-expressing tumors, we undertook our current research to find an optimum dose of amatuximab to neutralize the shed mesothelin and improve the tumor uptake of the antibody. We found in a nude mouse model of A431/K5 tumor (mesothelin-positive human epidermoid carcinoma cells) that the tumor uptake and blood retention of ^{111}In labeled amatuximab was inversely correlated to the tumor size, whereas the liver and spleen uptakes showed a positive correlation with tumor size [14]. However, we did not correlate the tumor and major organ uptakes with the concentration of circulating shed mesothelin since no methods to determine the shed mesothelin were available at the time the study of ^{111}In-labeled amatuximab was performed. In this current study, we used A431/H9 tumor as a model since we had previously determined that the serum concentration of shed mesothelin from this tumor positively correlated with tumor size [28]. The use of A431/H9 tumor enabled us not only to correlate tumor and the major organ uptake with the tumor size, but also to correlate tumor and the major organ uptake with the concentration of shed

mesothelin, thereby optimizing the injected dose of the antibody to neutralize the soluble antigen and to maximize the tumor uptake of the radiolabeled antibody.

The BD and PET imaging studies of ^{64}Cu-amatuximab in a mouse model of A431/H9 tumors demonstrated that the tumor uptake and blood retention of ^{64}Cu-amatuximab was inversely proportional to the tumor size whereas the liver uptake was positively correlated to the tumor size (Fig.2), similar to the results obtained previously with ^{111}In-amatuximab using A431/K5 tumors [14]. The PET imaging and uptake data from the ROI analysis of the images best illustrated the effect of amatuximab dose (2 vs. 60 μg) on the blood retention and the uptake of ^{64}Cu-amatuximab in tumor and major organs (Fig.4). The tumor uptake of the 2 and 60 μg amatuximab dose (%ID/g) was similar at 3 h p.i. Thereafter, drastic differences in blood retention, tumor, liver and spleen uptake of the radiolabel were observed between these two doses, especially at 24 h. For the first 24 h post-injection period, the radiolabel from 2 μg dose cleared very rapidly from blood without increasing the tumor uptake value (% ID/g), whereas the radiolabel from 60 μg cleared gradually from the blood and caused a drastic increase in tumor uptake value (% ID/g) at 24 h (Fig.4). These tumor uptake profiles are in contrast to the uptake profiles in the liver and spleen, which show much higher liver and spleen uptakes of the radiolabel for 2 μg dose than for 60 μg at 3 and 24 h p.i. However, the uptake values in liver and spleen became similar at 48 h between two doses.

These findings could be explained by correlating the uptake values with the concentration of the circulating shed mesothelin. Based on the uptake values calculated by the ROI analysis, the concentration of amatuximab (M.W, 144,330 Da) remaining in blood at 24 h is 0.69 nM for 2 μg injection because the blood concentration of amatuximab detected at 24 h was 5 %ID/g. Since the initial concentration of amatuximab after 2 μg injection is 8.7 nM in blood, assuming that the blood volume of a 20 g mouse is 1.6 ml (7.5% body weight) and the steady state concentration of shed mesothelin in blood is 4 nM for the tumor size (~200 mm^3) we used for the PET imaging study [28], the injected dose of 2 μg would mostly be bound to shed mesothelin in blood during the first 24 h after the injection, consequently sequestered into liver and spleen and therefore mostly unavailable to bind mesothelin expressed on the tumor surface during the first 24 h period. In comparison, the initial concentration of 60 μg in blood corresponds to 260 nM, which is at a large excess to the steady state concentration (4 nM) of shed mesothelin in blood and thus, a large portion of this injected dose was mostly unbound to the shed mesothelin in blood for the first 24 h and consequently distributed in the whole-body as free amatuximab available to bind shed mesothelin in the extracellular space of tumor or mesothelin expressed on tumor cell surface, thereby increasing the tumor uptake. The concentration of the antibody in blood at 24 h post-injection of 60 μg is estimated to be 54 nM (13 %ID/g), more than 10 fold greater than the initial steady state concentration (4 nM) of shed mesothelin in blood measured without amatuximab injection. However, it is interesting to note that the tumor uptake remained unchanged at 48 h and the tumor-to-liver and -spleen ratios from 60 μg dose also remained unchanged between 24 and 48 h p.i. This finding appears to indicate first that 54 nM of amatuximab remaining in blood at 24 h after the injection of 60 μg dose remained as mostly free amatuximab unbound to shed mesothelin in blood, thus not sequestered into the reticuloendothelial system in liver during the time between 24 and 48 h p.i. Secondly, it

appears that the tumor was already saturated with amsatuximab by 24 h, thus no additional accumulation of amatuximab occurred in the tumor at 48 h. Our current study demonstrated that for a nude mouse model of A431/H9 tumor, 30 to 60 fold excess amount of amatuximab to the steady state amount of shed mesothelin in blood could adequately neutralize the shed mesothelin in blood, thereby minimizing the liver uptake and maximizing the tumor uptake of the radiolabel.

Another important finding from the PET imaging study was that the images showed the highest concentration of the radiolabel localized in the tumor core when the images were obtained 24 and 48 h post-injection of 60 μg. Although our current study was not aimed at elucidation of the mechanism of the tumor microdistribution, the PET images suggest that the radiolabeled amatuximab diffused into extracellular space after crossing the tumor vasculature was mostly complexed with shed mesothelin in the extracellular space when 60 μg amatuximab dose was injected, thereby overcoming binding site barriers and the complex was distributed uniformly throughout the entire tumor by bypassing the binding sites on the surface of tumor cells nearest to the vasculature. The findings from the PET imaging studies are consistent with the results from a mathematical modeling by Pak, et al.[28]. This mathematical model predicted that the shed mesothelin in the extracellular space could provide a beneficial effect in distributing a mesothelin specific immunotoxin, SS1P (composed of the Fv portion of amatuximab and a truncated form of Pseudomonas exotoxin (PE38) uniformly in the entire solid tumor by overcoming the binding-site barriers. It is also very interesting to note that the PET images showed the highest concentration of the radiolabel from 60 μg amatuximab dose trapped in the tumor core at 24 and 48 h p.i. Further studies are required to define the mechanism of the trapping of the radiolabel in the tumor center. Although many more parameters still need to be defined, this study was the first important step to optimize the injected dose for individualized treatment of patients with mesothelin-positive tumors. We believe that amatuximab labeled with positron-emitters can further improve the sensitivity and resolution of tumor detection compared to the antibody labeled with a single photon such as ^{111}In. We previously investigated the use of ^{111}In labeled amatuximab to characterize the biodistribution, and dosimetry in patients with mesothelin-expressing cancers, four with malignant mesothelioma and two with pancreatic adenocarcinoma, by Single Photon Emission Computed Tomography-Computed Tomography (SPECT/CT) imaging [20]. We found that the radiotracer dose was well-tolerated and demonstrated physiologic uptake in the heart, liver, kidneys and spleen. The ^{111}In labeled amatuximab was localized to the primary and metastatic sites of mesothelin-expressing cancers. In all patients, tumor to background ratios (TBR) consistently met or exceeded an uptake of 1.2 (range 1.2–62.0) by 4 h p.i., which is the minimum TBR that can be visualized. The TBR increased further at 24–48 h with its value ranging from 1.5 to 9, indicating that the antibody labeled with ^{64}Cu (decay half-life, 12.7 h) would be useful in selecting patients with mesothelin expressing tumors for mesothelin-targeted therapies and monitoring response to such therapies.

5. Conclusion

The results of our studies provide a message that shed mesothelin in the circulation negatively affects the tumor uptake of the mesothelin-specific antibody, whereas shed

mesothelin in the extracellular space positively affects the tumor uptake by improving the microdistribution of the antibody, which is important for antibody-based therapy. Thus, our findings suggest that the injection of amatuximab dose which can saturate the shed mesothelin in blood and extracellular space would provide a beneficial effect not only in maximizing tumor uptake with minimum liver and spleen uptake, but also in distributing the radiolabel deeply into the tumor core. The high sensitivity and resolution of PET imaging enabled us to quantify the tumor and major organ uptake values of ^{64}Cu labeled amatuximab, which potentially have broad applicability in the clinical development of mesothelin-targeted therapies.

Acknowledgments

We thank Ms. Eden Dejene for her editorial assistance with this manuscript. This research was supported by the intramural research program of Clinical Center, NIH.

References

1. Wright BD, Lapi SE. Designing the magic bullet? The advancement of immuno-PET into clinical use. J Nucl Med. 2013; 54:1171–4. [PubMed: 23908265]
2. Pecking AP, Bellet D, Alberini JL. Immuno-SPET/CT and immuno-PET/CT: a step ahead to translational imaging. Clinical & experimental metastasis. 2012; 29:847–52. [PubMed: 22760521]
3. van Dongen GA, Poot AJ, Vugts DJ. PET imaging with radiolabeled antibodies and tyrosine kinase inhibitors: immuno-PET and TKI-PET. Tumour biology : the journal of the International Society for Oncodevelopmental Biology and Medicine. 2012; 33:607–15. [PubMed: 22270450]
4. Lawrentschuk N, Davis ID, Bolton DM, Scott AM. Positron emission tomography (PET), immuno-PET and radioimmunotherapy in renal cell carcinoma: a developing diagnostic and therapeutic relationship. BJU international. 2006; 97:916–22. [PubMed: 16643471]
5. Verel I, Visser GW, van Dongen GA. The promise of immuno-PET in radioimmunotherapy. J Nucl Med. 2005; 46 (Suppl 1):164S–71S. [PubMed: 15653665]
6. Qin C, Liu H, Chen K, Hu X, Ma X, Lan X, et al. Theranostics of malignant melanoma with 64CuCl2. J Nucl Med. 2014; 55:812–7. [PubMed: 24627435]
7. Wiehr S, Buhler P, Gierschner D, Wolf P, Rolle AM, Kesenheimer C, et al. Pharmacokinetics and PET imaging properties of two recombinant anti-PSMA antibody fragments in comparison to their parental antibody. The Prostate. 2014; 74:743–55. [PubMed: 24610028]
8. Chen X, Liu S, Hou Y, Tohme M, Park R, Bading JR, et al. MicroPET imaging of breast cancer alphav-integrin expression with 64Cu-labeled dimeric RGD peptides. Mol Imaging Biol. 2004; 6:350–9. [PubMed: 15380745]
9. Bryan JN, Jia F, Mohsin H, Sivaguru G, Anderson CJ, Miller WH, et al. Monoclonal antibodies for copper-64 PET dosimetry and radioimmunotherapy. Cancer biology & therapy. 2011; 11:1001–7. [PubMed: 21464612]
10. Holland JP, Caldas-Lopes E, Divilov V, Longo VA, Taldone T, Zatorska D, et al. Measuring the pharmacodynamic effects of a novel Hsp90 inhibitor on HER2/neu expression in mice using Zr-DFO-trastuzumab. PloS one. 2010; 5:e8859. [PubMed: 20111600]
11. Wu AM. Antibodies and antimatter: the resurgence of immuno-PET. J Nucl Med. 2009; 50:2–5. [PubMed: 19091888]
12. Bhattacharyya S, Kurdziel K, Wei L, Riffle L, Kaur G, Hill GC, et al. Zirconium-89 labeled panitumumab: a potential immuno-PET probe for HER1-expressing carcinomas. Nucl Med Biol. 2013; 40:451–7. [PubMed: 23454247]
13. Holland JP, Divilov V, Bander NH, Smith-Jones PM, Larson SM, Lewis JS. 89Zr-DFO-J591 for immunoPET of prostate-specific membrane antigen expression in vivo. J Nucl Med. 2010; 51:1293–300. [PubMed: 20660376]

14. Shin IS, Lee SM, Kim HS, Yao Z, Regino C, Sato N, et al. Effect of chelator conjugation level and injection dose on tumor and organ uptake of 111In-labeled MORAb-009, an anti-mesothelin antibody. Nucl Med Biol. 2011; 38:1119–27. [PubMed: 21741258]
15. Hassan R, Cohen SJ, Phillips M, Pastan I, Sharon E, Kelly RJ, et al. Phase I clinical trial of the chimeric anti-mesothelin monoclonal antibody MORAb-009 in patients with mesothelin-expressing cancers. Clin Cancer Res. 2010; 16:6132–8. [PubMed: 21037025]
16. Hassan R, Ebel W, Routhier EL, Patel R, Kline JB, Zhang J, et al. Preclinical evaluation of MORAb-009, a chimeric antibody targeting tumor-associated mesothelin. Cancer immunity. 2007; 7:20. [PubMed: 18088084]
17. Kelly RJ, Sharon E, Pastan I, Hassan R. Mesothelin-targeted agents in clinical trials and in preclinical development. Molecular cancer therapeutics. 2012; 11:517–25. [PubMed: 22351743]
18. Chang K, Pastan I, Willingham MC. Isolation and characterization of a monoclonal antibody, K1, reactive with ovarian cancers and normal mesothelium. Int J Cancer. 1992; 50:373–81. [PubMed: 1735605]
19. Chang K, Pastan I. Molecular cloning of mesothelin, a differentiation antigen present on mesothelium, mesotheliomas, and ovarian cancers. Proc Natl Acad Sci U S A. 1996; 93:136–40. [PubMed: 8552591]
20. Lindenberg L, Thomas A, Adler S, Mena E, Kurdziel K, Maltzman J, et al. Safety and biodistribution of 111In-amatuximab in patients with mesothelin expressing cancers using single photon emission computed tomography-computed tomography (SPECT-CT) imaging. Oncotarget. 2015; 6:4496–504. [PubMed: 25756664]
21. Zhang Y, Hansen JK, Xiang L, Kawa S, Onda M, Ho M, et al. A flow cytometry method to quantitate internalized immunotoxins shows that taxol synergistically increases cellular immunotoxins uptake. Cancer Res. 2010; 70:1082–9. [PubMed: 20103626]
22. Zhang Y, Xiang L, Hassan R, Pastan I. Immunotoxin and Taxol synergy results from a decrease in shed mesothelin levels in the extracellular space of tumors. Proc Natl Acad Sci U S A. 2007; 104:17099–104. [PubMed: 17940013]
23. Bradford MM. A rapid and sensitive method for the quantitation of microgram quantities of protein utilizing the principle of protein-dye binding. Anal Biochem. 1976; 72:248–54. [PubMed: 942051]
24. Lindmo T, Bunn PA Jr. Determination of the true immunoreactive fraction of monoclonal antibodies after radiolabeling. Methods Enzymol. 1986; 121:678–91. [PubMed: 3523136]
25. Weldon JE, Xiang L, Zhang J, Beers R, Walker DA, Onda M, et al. A recombinant immunotoxin against the tumor-associated antigen mesothelin reengineered for high activity, low off-target toxicity, and reduced antigenicity. Molecular cancer therapeutics. 2013; 12:48–57. [PubMed: 23136186]
26. Bao Q, Newport D, Chen M, Stout DB, Chatziioannou AF. Performance evaluation of the inveon dedicated PET preclinical tomograph based on the NEMA NU-4 standards. J Nucl Med. 2009; 50:401–8. [PubMed: 19223424]
27. Zhang Y, Hong H, Engle JW, Bean J, Yang Y, Leigh BR, et al. Positron emission tomography imaging of CD105 expression with a 64Cu-labeled monoclonal antibody: NOTA is superior to DOTA. PloS one. 2011; 6:e28005. [PubMed: 22174762]
28. Pak Y, Pastan I, Kreitman RJ, Lee B. Effect of antigen shedding on targeted delivery of immunotoxins in solid tumors from a mathematical model. PloS one. 2014; 9:e110716. [PubMed: 25343405]

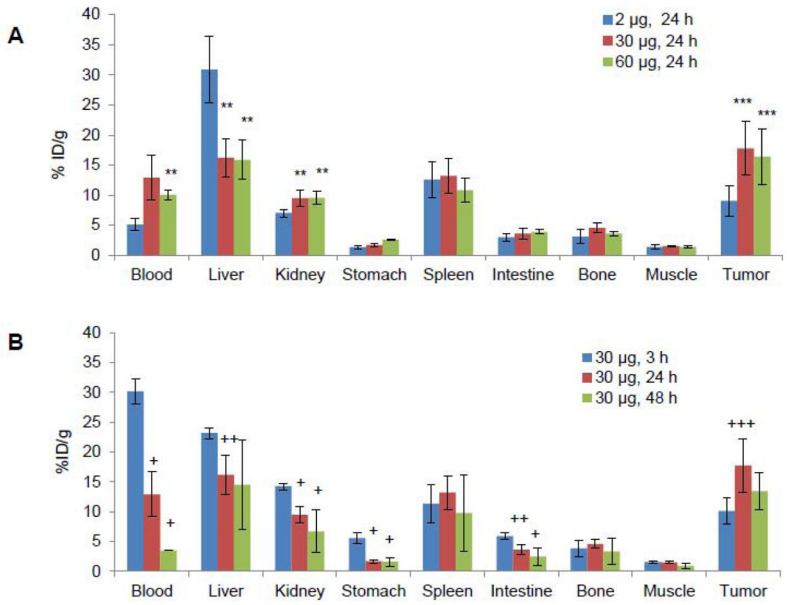

Figure 1.

Effects of total injection dose of amatuximab on the biodistribution of ^{64}Cu-NOTA-amatuximab in nude mice with tumor size ~200 mm^3 (range, 80~300 mm^3). (A) The bidodistribution data from ^{64}Cu-NOTA-amatuximab with different injection doses (10 μCi/2 μg, 10 μCi/30 μg, and 10 μCi/60 μg) are compared at 24 h p.i. in different organs, demonstrating that tumor uptake significantly increased and the liver uptake decreased when the injection dose was above 30 μg. (B) The biodistribution of ^{64}Cu-NOTA-amatuximab at different post-injection times. The maximum tumor uptake of ^{64}Cu-NOTA-amatuximab (10 μCi) was shown at 24 h post-injection when coinjected with 30 μg amatuximab. The data are mean ± S.D. (n = 5). Analysis of statistical significance in each organ uptake data (A) compared to the data from 2 μg injection and (B) compared to the data from 3 h p.i.: *P<0.001, **0.001<P<0.01, ***0.01<P<0.05; ^{+}P<0.001, $^{++}$0.001<P<0.01, $^{+++}$0.01<P<0.05. Column, mean; bar, S.D.

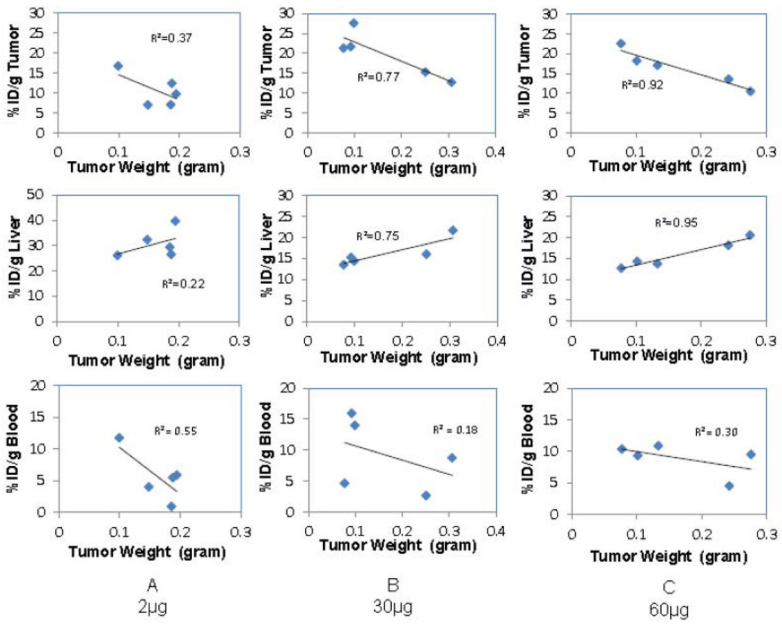

Figure 2.

Effects of tumor size and total injection dose of amatuximab on biodistribution of ^{64}Cu-NOTA-amatuximab (10 μCi) at one day p.i.: A) 2 μg, B) 30 μg, and C) 60 μg. The relationship between tumor size and tumor uptake, between tumor size and liver uptake, and between tumor size and blood retention are plotted, demonstrating a positive correlation between tumor size and liver uptake, but an inverse correlation between tumor size and tumor uptake and between tumor size and blood retention.

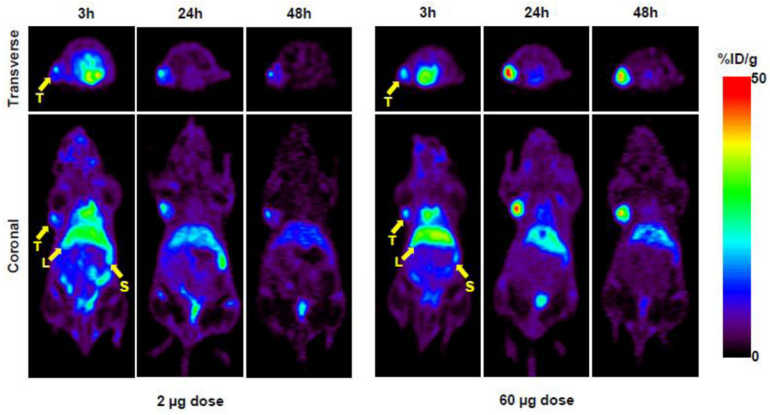

Figure 3.

Representative transverse and coronal PET images of ^{64}Cu-NOTA-amatuximab (0.3 mCi) coinjected with 2 μg and 60 μg amatuximab at 3, 24, and 48 h p.i. in nude mice with tumor size ~200 mm^3 (range, 170 to 320 mm^3). PET images demonstrate that tumor uptake significantly increased when injection dose was 60 μg. T, tumor; L, liver; S, spleen.

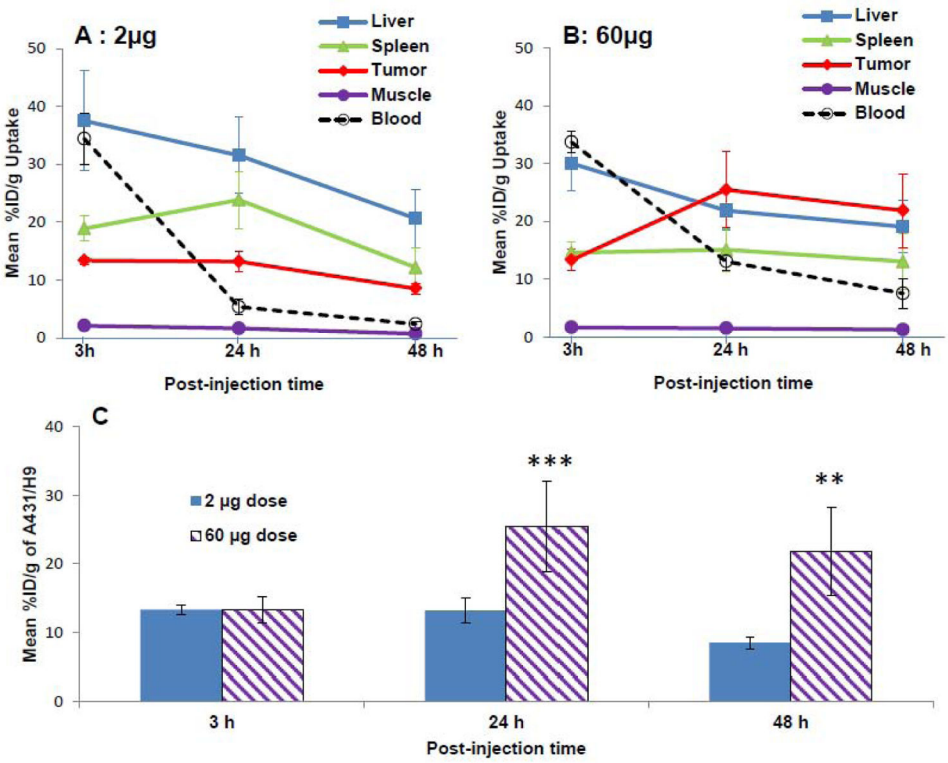

Figure 4.

Effect of amatuximab dose (2 μg and 60 μg) on accumulation of ^{64}Cu-NOTA-amatuximab (0.3 mCi) in tumor, blood and organs in nude mice with tumor size ~200 mm^3 (range, 170~320 mm^3). The uptake value (% ID/g) was calculated by ROI analysis of PET images. (A) time activity curves for tumor, liver, blood, spleen and muscle from 2 μg injection and (B) from 60 μg injection; and (C) comparison of tumor uptake of ^{64}Cu-NOTA-amatuximab coinjected with 2 μg and 60 μg amatuximab. Analysis of statistical significance in tumor uptake data from 6 μg dose compared to the data from 2 μg dose. **0.001<*P*<0.01, ***0.01<*P*<0.05.

Table 1

Effect of amatuximab dose (2, 30 and 60 μg) on tumor-to-blood and tumor-to-organ uptake ratios of ^{64}Cu-NOTA- amatuximab (10 μCi) in nude mice with tumor size ~200 mm^3 (range, 80~300 mm^3). All values are reported as mean ± standard deviation (n=5).

Time	Injection Dose	Tumor/Blood	Tumor/Liver	Tumor/kidney	Tumor/Spleen	Tumor/Muscle
24hr	2μg	3.00 ± 2.75	0.36 ± 0.19	1.48 ± 0.45	0.76 ± 0.41	8.83 ± 3.43
24hr	30μg	3.02 ± 2.00	1.29 ± 0.52	2.06 ± 0.44	1.58 ± 0.69	12.93 ± 3.90
24hr	60μg	1.96 ± 0.71	1.11± 0.50	1.70 ± 0.36	1.52 ± 0.33	11.85 ± 3.45
3hr	30μg	0.33 ± 0.06	0.44 ± 0.09	0.71± 0.15	0.95± 0.33	6.58 ± 1.71
48hr	30μg	6.43 ± 3.1	0.88 ± 0.43	1.92 ± 1.01	1.50 ± 1.19	14.41± 8.02

Table 2

Effect of amatuximab dose (2 vs. 60 μg) on tumor-to-blood and tumor-to-organ uptake ratios of ^{64}Cu-NOTA- amatuximab (0.3 mCi) in nude mice with tumor size ~200 mm^3 (range, 170~320 mm^3). The ratios were calculated by mean uptake values from ROI analysis of PET images. Blood-H represents the blood activity in the heart. All values are reported as mean ± standard deviation (n=5).

Time	Injection Dose	Tumor/Liver	Tumor/Spleen	Tumor/Muscle	Tumor/Blood_H
3hr	2μg	0.37 ± 0.08	0.72 ± 0.10	6.47 ± 1.19	0.39 ± 0.06
24hr	2μg	0.44 ± 0.17	0.58 ± 0.20	8.26 ± 1.53	2.62 ± 0.87
48hr	2μg	0.44 ± 0.15	0.76 ± 0.26	12.32 ± 2.18	3.67 ± 0.48
3hr	60μg	0.45 ± 0.03	0.91 ± 0.04	7.86 ± 0.82	0.39 ± 0.03
24hr	60μg	1.16 ± 0.20	1.70 ± 0.34	16.46 ± 4.62	1.93 ± 0.39
48hr	60μg	1.18 ± 0.44	1.78 ± 0.70	17.26 ± 6.36	3.13 ± 1.45